



Research Article

Biochemical characterization of the recombinant schistosome tegumental protein SmALDH_312 produced in *E. coli* and baculovirus expression vector system



Julie Harnischfeger^{a,#}, Mandy Beutler^{b,#}, Denise Salzig^a, Stefan Rahlfs^c, Katja Becker^c, Christoph G. Grevelding^b, Peter Czermak^{a,d,*}

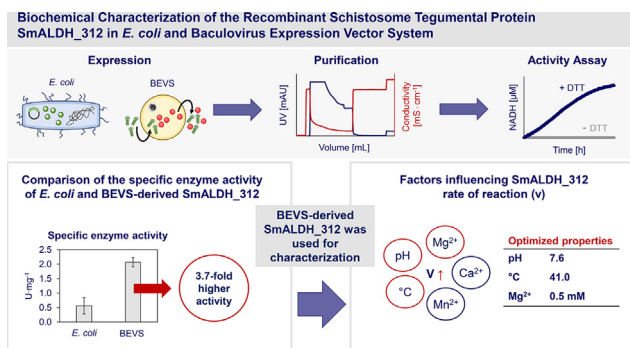
^a Institute of Bioprocess Engineering and Pharmaceutical Technology, University of Applied Sciences Mittelhessen, Giessen, Germany

^b Institute for Parasitology, Biomedical Research Centre, Justus Liebig University Giessen, Giessen, Germany

^c Biochemistry and Molecular Biology, Interdisciplinary Research Centre Giessen, Justus Liebig University Giessen, Giessen, Germany

^d Faculty of Biology and Chemistry, Justus Liebig University Giessen, Giessen, Germany

GRAPHICAL ABSTRACT



ARTICLE INFO

Article history:

Received 29 January 2021

Accepted 12 August 2021

Available online 17 August 2021

Keywords:

Activity assay

Aldehyde dehydrogenase

Baculovirus expression vector system

Drug targets

Escherichia coli

Metal ions

Parasitic proteins

Recombinant protein expression

Recombinant Schistosome Tegumental

Protein

ABSTRACT

Background: The heterologous expression of parasitic proteins is challenging because the sequence composition often differs significantly from host preferences. However, the production of such proteins is important because they are potential drug targets and can be screened for interactions with new lead compounds. Here we compared two expression systems for the production of an active recombinant aldehyde dehydrogenase (SmALDH_312) from *Schistosoma mansoni*, which causes the neglected tropical disease schistosomiasis.

Results: We produced SmALDH_312 successfully in the bacterium *Escherichia coli* and in the baculovirus expression vector system (BEVS). Both versions of the recombinant protein were found to be active *in vitro*, but the BEVS-derived enzyme showed 3.7-fold higher specific activity and was selected for further characterization. We investigated the influence of Mg²⁺, Ca²⁺ and Mn²⁺, and found out that the specific activity of the enzyme increased 1.5-fold in the presence of 0.5 mM Mg²⁺. Finally, we characterized the kinetic properties of the enzyme using a design-of-experiment approach, revealing optimal activity at pH 7.6 and 41°C.

Conclusions: Although, *E. coli* has many advantages, such as rapid expression, high yields and low costs, this system was outperformed by BEVS for the production of a schistosome ALDH. BEVS therefore

Peer review under responsibility of Pontificia Universidad Católica de Valparaíso

* Corresponding author.

E-mail address: peter.czermak@lse.thm.de (P. Czermak).

These authors contributed equally to this work.

<https://doi.org/10.1016/j.ejbt.2021.08.002>

0717-3458/© 2021 Pontificia Universidad Católica de Valparaíso. Production and hosting by Elsevier B.V.

This is an open access article under the CC BY-NC-ND license (<http://creativecommons.org/licenses/by-nc-nd/4.0/>).

Schistosoma mansoni

provides an opportunity for the expression and subsequent evaluation of schistosome enzymes as drug targets.

How to cite: Harnischfeger J, Beutler M, Salzig D, et al. Biochemical characterization of the recombinant schistosome tegumental protein SmALDH_312 produced in *E. coli* and baculovirus expression vector system. Electron J Biotechnol 2021;54. <https://doi.org/10.1016/j.ejbt.2021.08.002>

© 2021 Pontificia Universidad Católica de Valparaíso. Production and hosting by Elsevier B.V. This is an open access article under the CC BY-NC-ND license (<http://creativecommons.org/licenses/by-nc-nd/4.0/>).

1. Introduction

The expression of parasite proteins in heterologous systems such as the bacterium *Escherichia coli*, or eukaryotic systems such as yeast and Chinese hamster ovary (CHO) cells, is often challenging because the base composition and codon preferences of the corresponding genes differ significantly among hosts. For example, genes from the malaria parasite *Plasmodium falciparum* have a typical base composition of ~80 % AT compared to an average of ~59% of mammals [1,2,3], which means that codon optimization is necessary to ensure the efficient expression of *Plasmodium* genes in animal cells [4]. Similarly, genes from multicellular parasites such as *Schistosoma mansoni* typically have a base composition of 62–66% A/T [5,6,7,8] thus may require codon optimization for heterologous expression [9]. However, codon optimization does not guarantee a more efficient translation in *E. coli* [10]. Just as in *E. coli*, codon optimization does not necessarily evoke an improvement in protein expression. Since the BEVS possesses a robust codon usage, coding sequences of most species can normally be expressed in insect cells [11]. Many parasite enzymes also require post-translational modifications (PTMs), such as phosphorylation, which is necessary for signaling in *S. mansoni* [12]. The modification of cysteine residues also plays a decisive role in host invasion, including cysteine palmitoylation in *P. falciparum* and *Toxoplasma gondii* [11]. As in other eukaryotes, *S. mansoni* are able to do typical PTMs such as sumoylation, ubiquitination, NEDDylation, farnesylation, glycosylation, acetylation, and phosphorylation [12,13,14,15,16,17,18,19]. Further oxidative modifications are required to optimize protein folding via the formation of disulfide bonds and to regulate redox reactions and signal transduction [20,21]. Thus, *S. mansoni* possesses a thioredoxin peroxidase-1, which causes a disulfide-mediated protein folding [21,22]. Furthermore, it is important to find a suitable production platform for parasite enzymes because they are potential drug targets for the treatment of parasitic diseases.

We have focused on the production of enzymes from *S. mansoni* because this blood fluke infects ~240 million people worldwide [23] and schistosomiasis has been defined by the WHO as a neglected tropical disease (NTD) [24]. There is no vaccine against *S. mansoni* and only one drug (Praziquantel) is approved as general schistosomicide, creating an urgent need for alternative treatment options [25]. Accordingly, research has focused on the identification and characterization of genes that fulfil important functions in schistosome biology, and that may encode drug targets or potential vaccine antigens [26]. Progress is dependent on the effective production of recombinant schistosome proteins.

Several schistosome proteins have been expressed in *E. coli*, particularly in the widely used production strain BL21(DE) and its derivatives [27]. For example, *E. coli* strains BL21(DE) and BL21(DE)pLysS have been used to produce *S. japonicum* aldose reductase (believed to be involved in antioxidant defense) and the *S. japonicum* and *S. mansoni* anti-inflammatory proteins Sj16 and Sm16 [28,29,30]. *E. coli* is preferable because it is a well-established and inexpensive platform, but it is unsuitable for complex proteins and those requiring PTMs. Yeast such as *Saccharomyces cerevisiae* provide an alternative to address the

limitations of bacteria, but not all schistosome proteins are efficiently expressed in yeast. For example, five integrin receptors have been identified in *S. mansoni* [31] but only the β integrin receptor 1 was expressed in *S. cerevisiae*, whereas premature transcriptional termination prevented in the expression of the four α integrin receptors 1–4, because the AT-rich sequences were misinterpreted by the mRNA processing machinery [32]. Yeast can introduce PTMs such as phosphorylation, acetylation, glycosylation and disulfide bonds, but misfolding may still occur due to conformational stress [33]. Other expression systems are therefore required for such complex proteins. For example, the baculovirus expression vector system (BEVS) involves the use of insect cells, which are advantageous because they fold complex proteins and introduce PTMs similar to those found in mammals, and with similar efficiency [34]. Therefore BEVS offers a promising alternative for the production of complex schistosome proteins, as already been demonstrated by the successful expression of the tegumental proteins Sm23 and Sm-p80 [35,36].

Here we compared the well-established *E. coli* system and BEVS to determine their suitability for the production of schistosome enzymes as potential drug targets (Fig. 1). To this end, we generated functional versions of the *S. mansoni* aldehyde dehydrogenase SmALDH_312 (GeneID: Smp_312440; previously Smp_050390), which is interesting as a potential drug target due to its localization in the tegument [37]. To the best of our knowledge, this enzyme has not yet been expressed in a heterologous system and its kinetic properties have not been explored. Therefore, we used an *in vitro* activity assay to compare the suitability of the two expression systems and characterized the kinetic properties of the recombinant enzyme in order to increase its activity in functional screening assays to identify potential drug leads.

2. Materials and methods

2.1. *E. coli* protein expression strains

For expression of SmALDH_312 we selected *E. coli* strains BL21 (DE3)[pLysS] (referred in this paper as pLysS, Promega, Walldorf, Germany) and BL21(DE3)LOBSTR-RIL (referred as LOBSTR-RIL, Kerfast, Boston, MA, USA). The advantage of pLysS is the expression of T7 lysozyme, which allows a tight control of protein expression. It does not interfere with protein expression following induction by isopropyl β -D-1-thiogalactopyranoside (IPTG). Advantages of the LOBSTR-RIL strain are the co-expression of rare tRNAs as arginine (R), isoleucine (I) and leucine (L) as well as modifications in Arna and SlyD, polyhistidine rich proteins, which are considerably less co-purified by His-tag affinity purification.

2.2. Recombinant protein expression in *E. coli*

2.2.1. Cloning the SmALDH_312 construct

Total RNA was isolated by homogenizing individual worms in 500 μ L peqGOLD TriFast (PEQLAB Biotechnologie, Erlangen, Germany) followed by chloroform extraction and ethanol precipitation according to the manufacturer's instructions. First strand cDNA was synthesized using the QuantiTect Reverse Transcription Kit

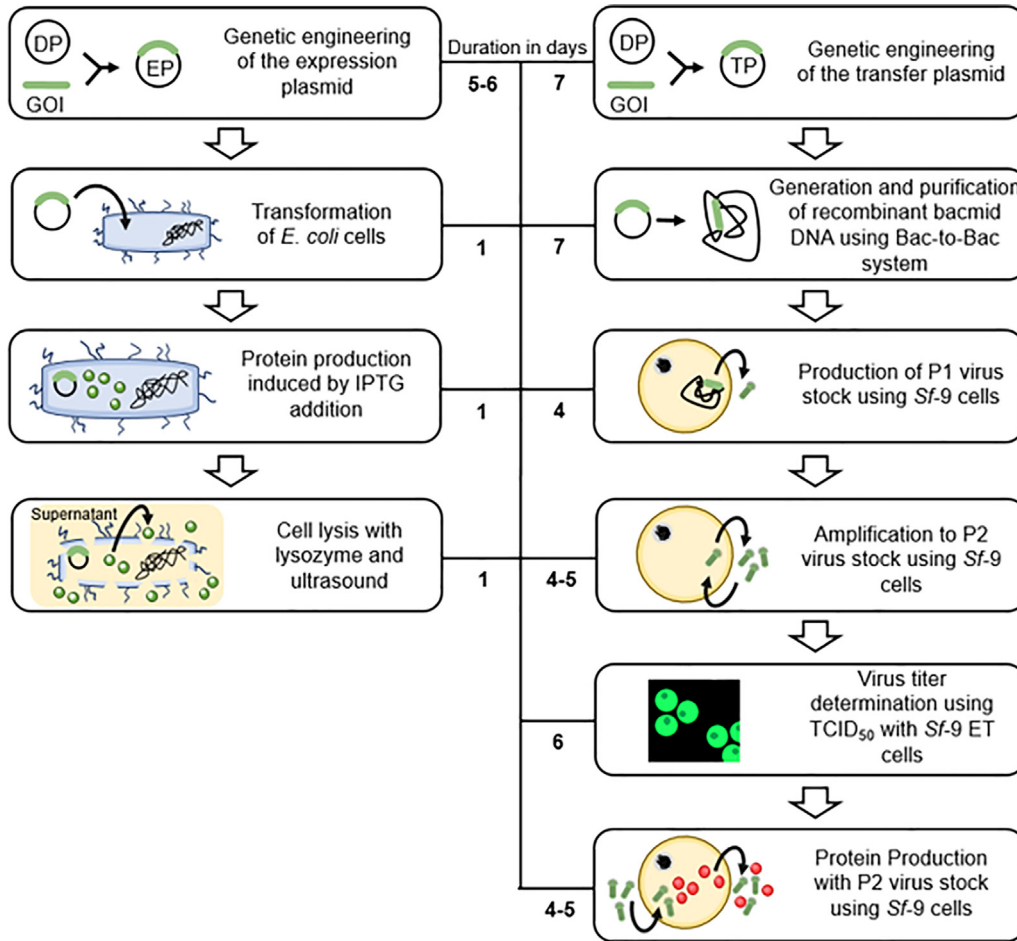


Fig. 1. Comparison of protein production in *Escherichia coli* system (left), which requires ~9 days, and the baculovirus expression system (right), which requires 34–36 d.

(Qiagen, Hilden, Germany) according to the manufacturer's instructions. Full-length cDNA was amplified with primers designed to introduce 5' NdeI and 3' NotI sites and a 3' His₆ tag (forward primer: 5'-TTT Tca tat gAC GAA GAC ATA TCG TCT TCC CGA AG-3' and reverse primer: 5'-AAA Agc ggc cgc TTA ATG GTG ATG GTG ATG GTG AGA GTT CTT TAC TGA AAT TGG CAT AGA AAT CAC-3'; switch to lower case indicates restriction site) using AccuPrime TaqDNA Polymerase High Fidelity (Invitrogen Ltd, Paisley, UK). The product was purified by agarose gel electrophoresis and extracted using NucleoSpin™ Gel and PCR Clean-up Kit (Macherey-Nagel, Düren, Germany). The SmALDH₃₁₂ cDNA insert and vector pET-30a(+) (Merck KGaA, Darmstadt, Germany) were digested with NdeI (New England Biolabs, Massachusetts, USA) and NotI (New England Biolabs) and ligated at a 3:1 ratio with T4 DNA ligase (New England Biolabs). The final vector pET-30a-SmALDH₃₁₂ (Fig. 2) was stored at -20°C.

2.2.2. Transformation of *E. coli*

NEB 5-α (a strain for efficient cloning, New England Biolabs), pLysS and LOBSTR-RIL competent *E. coli* cells were transformed by heat shock according to the manufacturer's recommendations and spread on LB agar plates containing 50 μg·mL⁻¹ kanamycin (Carl Roth, Karlsruhe, Germany) before incubating at 37°C overnight. For the protein expression strains, the agar plates also included 50 μg·mL⁻¹ chloramphenicol (Carl Roth). The next day, colonies were picked and transferred to a master plate, which was incubated at 37°C overnight. Single colonies were then inoculated into 50-mL Erlenmeyer flasks containing 20 mL LB medium supplemented with 50 μg·mL⁻¹ kanamycin and incubated at

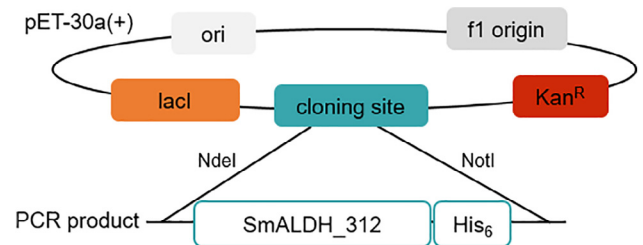


Fig. 2. Cloning of SmALDH₃₁₂ for the *Escherichia coli* expression system. The full-length SmALDH₃₁₂ sequence was amplified by PCR using primers that introduced a 5' NdeI site and a 3' NotI site. The insert and vector pET-30a(+) were digested with NdeI and NotI before ligation to produce the final vector pET-30a-SmALDH₃₁₂.

37°C overnight, shaking at 180 rpm. Bacterial cells were then pelleted and plasmid DNA was isolated using the GeneJET Plasmid Miniprep Kit (Thermo Fisher Scientific, Waltham Massachusetts, USA). DNA quality and quantity were determined by spectrophotometry using a BioPhotometer Plus 6132 (Eppendorf AG, Hamburg, Germany) and the pET-30a-SmALDH₃₁₂ vector was then sequenced by LGC Genomics (Berlin, Germany). The corresponding bacterial colony was stored in 50% (v/v) glycerol.

2.2.3. Expression of SmALDH₃₁₂ in *E. coli*

For the expression kinetics, pre-cultures of *E. coli* strains pLysS and LOBSTR-RIL were prepared in 20 mL LB medium containing 50 μg·mL⁻¹ kanamycin and 50 μg·mL⁻¹ chloramphenicol by inocu-

lation with a single colony from an agar plate and incubating at 37°C overnight, shaking at 180 rpm. Overnight cultures were diluted to an OD₆₀₀ of 0.1 into 50 mL LB medium (main culture) and incubated as above until the OD₆₀₀ reached 0.6–0.8. Recombinant protein expression was induced by adding 200 µM IPTG (Carl Roth) and incubating at room temperature (RT) for up to 19 h, shaking at 180 rpm. Samples were taken every hour until 4 h past induction and 19 h past induction. For protein production the main culture volume was adjusted to 400 mL LB Medium. Cells were harvested 4 h post induction by centrifugation (8,000 × g, 15 min, 4°C) and stored at –20°C overnight. The next day, the bacterial cell pellet was resuspended in lysis buffer (100 mM Tris, pH 7.4; 10 mM imidazole) and lysed by adding 100,000 U lysozyme (Sigma-Aldrich, Inc., St. Louis, USA) per gram of biomass, 10 µg·mL⁻¹ RNase (Carl Roth), 10 µg·mL⁻¹ DNase I (Sigma-Aldrich) and SIGMAFAST Protease Inhibitor Cocktail Tablet (Sigma-Aldrich) and shaking gently for 1 h at 4°C. The samples were sonicated on ice (3 × 1 min, alternating on/off pulses of 1 s at 60% power), pelleted by centrifugation (18,000 × g, 30 min, 4°C) and the supernatant was passed through a 0.2 µm polyethersulfone (PES) membrane (Carl Roth) into a 50-mL centrifuge tube.

2.3. Recombinant protein expression using BEVS

2.3.1. Preparation of the baculovirus vector

We used the Bac-to-Bac system including competent *E. coli* strain DH10Bac and the vector pFastBac 1 (Thermo Fisher Scientific). The expression cassette, prepared by GeneArt Gene Synthesis (Thermo Fisher Scientific) comprised the very late polyhedrin promoter (polh), a N-terminal His₆-tag, the GP64 signal sequence, a thrombin cleavage site (Thr_C), the full-length cDNA sequence of SmALDH₃₁₂ and the SV40 polyadenylation site. Transformation of component *E. coli* cells was carried out according to the manufacturer's instructions and the bacmid DNA was purified and stored as previously described [38]. The final vector and its integration site in the baculovirus genome are shown in Fig. 3.

2.3.2. Production of recombinant baculoviruses

Recombinant baculoviruses were produced in the *Spodoptera frugiperda* cell line Sf-9. We seeded 6·10⁵ cells·mL⁻¹ Sf-9 TriEx cells (Merck) into each well of a six-well plate in 2 mL Sf-900 II serum-free media (SFM; Thermo Fisher Scientific) and incubated the plate overnight at 28°C without shaking. The next day, we prepared transfection mixtures for each well by mixing 2.5 µg bacmid DNA with 250 µL Grace's insect medium (Sigma-Aldrich) in 1-mL centrifuge tubes. The tubes were inverted 10 times. Before adding the transfection mixture dropwise to the cell suspension, 5 µL of the transfection reagent TransIT-Insect reagent (Mirus Bio, Madison, WI, USA) was added to each transfection mixture. Following a further incubation as above for 72 h, the cell suspension was

transferred to 15-mL sterile centrifuge tubes and centrifuged at 1,000 × g for 5 min at RT. The supernatant, containing P1 virus stock, was transferred to fresh, sterile 15-mL dark centrifuge tubes and stored at 4°C.

2.3.3. Amplification and titration of recombinant baculoviruses

Sf-9 TriEx cells were seeded in 48 mL Sf-900 II SFM in a 250-mL baffled shake flask wrapped in aluminium foil to avoid light, and 2 mL of the P1 virus stock prepared above was added to bring the final volume to 50 mL, making an initial cell density of 1.0·10⁶ cells·mL⁻¹. The cells were incubated until the viability fell to ~70%, as determined using a guava easyCyte 6HT-2L flow cytometer (Luminex, Austin, Texas) with propidium iodide 4.5 mg·L⁻¹ (Sigma-Aldrich). When the cell viability fell to ~60%, the cells were transferred to a 50-mL tube and the P2 virus stock was harvested by centrifugation (250 × g for 10 min, RT) followed by transferring the supernatant to a fresh tube and a second centrifugation step (3,000 × g for 10 min, RT). The supernatant was transferred to a dark 50-mL centrifuge tube and stored at 4°C. The TCID₅₀ was determined using Sf-9 Easy Titer Cell Line (Kerafast, Boston, Massachusetts, USA) according to the manufacturer's protocol.

2.4. Production and purification of SmALDH₃₁₂

For initial testing, a fresh 1 L shake-flask culture of Sf-9 cells with a density of 1·10⁶ c·mL⁻¹ was infected with the P2 virus stock to a multiplicity of infection (MOI) of 0.01. The culture was sampled regularly over 72 h, with cell pellets and supernatants tested separately to confirm the product was secreted. The cell pellets were solubilized in lysis buffer (50 mM Tris, pH 7.8, 150 mM NaCl, 1% (v/v) Nonidet P-40) before testing. To purify the secreted recombinant protein, the supernatant was passed through a 0.2 µm PES filter to remove particulates and the cleared solution was applied to a HisTrap HP column (*E. coli*-derived enzyme) and HisTrap excel column (BEVS-derived SmALDH₃₁₂; GE Healthcare, Chicago, Illinois, USA) on an ÄKTA start fast protein liquid chromatography system (GE Healthcare). The pure enzyme was eluted in a gradient of up to 300 mM imidazole (Sigma-Aldrich) for the *E. coli* product and 500 mM imidazole for the BEVS product. The *E. coli*-derived enzyme was then concentrated using Vivaspın 20 (Merck) with a MWCO of 30 kDa and PES membrane. After, the *E. coli* and the BEVS products were rebuffed in 100 mM Tris-HCl (pH 7.5) using a Bio-Scale Mini Bio-Gel (Bio-Rad Laboratories, Hercules, California, USA).

2.5. Determination of protein concentration, recovery rate and relative purity

The recovery rate was determined by a western blot using the quantity tool of the analysis software Image Lab 6.0.1 (Bio-Rad Laboratories). The protein concentration was determined using bicinchoninic acid (BCA) assay (Thermo Fisher Scientific) according to the manufacturer's instructions. Protein yield and purity were determined using 4–20% Criterion TGX Stain-Free Protein Gels (Bio-Rad Laboratories), which possess the advantage of analysing the SDS-gel within a few minutes after running the SDS-PAGE. A densitometric analysis using Image Lab 6.0.1 was followed to compare the bands with a known enzyme concentration.

2.6. Activity assay

Aldehyde dehydrogenases such as SmALDH₃₁₂ catalyze the conversion of acetaldehyde to acetic acid while consuming NAD⁺ to NADH, as shown in Equation 1.

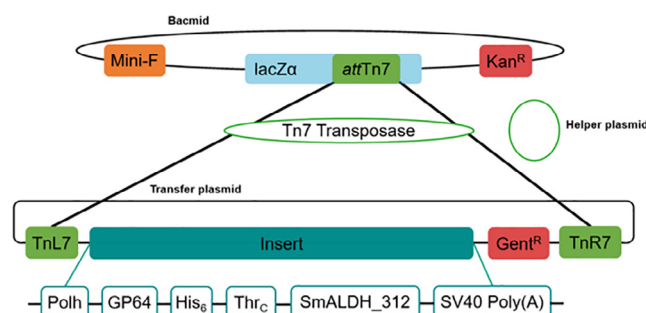


Fig. 3. Integration of the BEVS expression vector into the baculovirus genome by site-specific transposition, mediated by a transposase provided in *trans* by a helper plasmid. Integration was induced in *E. coli* DH10Bac cells carrying the corresponding bacmid.

Under specific conditions (pH = 7.5; T = 37°C) kinetic analysis was carried out using 33.3 μM acetaldehyde (Carl Roth), 33.3 μM NAD⁺ (Carl Roth) and 167 nM SmALDH_312. We also carried out tests at a range of enzyme concentrations (83–500 nM) and with various concentrations (1–10 mM) dithiothreitol (DTT). The formation of NADH was measured continuously by spectrophotometry at 340 nm. The NADH concentration was determined using a seven-point calibration line.

The activity of the SmALDH_312 was defined as shown in Equation 2, with 1 unit (*U*) representing the turnover of 1 nmol NADH per minute. The calculation is based on the change of NADH concentration (ΔC) in relation to the total reaction volume (*V*) over the change in time (ΔT).

$$U \left[\text{nmol} \cdot \text{min}^{-1} \right] = ((\Delta C) \cdot V) / (\Delta T) \quad \text{Equation 2}$$

The specific enzyme activity was calculated by including the amount of protein used, as shown in Equation 3.

$$U \cdot \text{mg}^{-1} \left[\text{nmol} \cdot \text{min}^{-1} \cdot \text{mg}^{-1} \right] = ((\Delta C) \cdot V) / ((\Delta T) \cdot \text{mg}_{\text{SmALDH}_312}) \quad \text{Equation 3}$$

All kinetic analysis was carried out in technical triplicates, and curves were fitted using OriginPro v9.0 (OriginLab, Northampton, MA, USA).

2.7. Characterization and optimal reaction conditions

The influence of Mg²⁺, Ca²⁺ and Mn²⁺ on enzyme activity was determined by kinetic analysis using 33.3 μM acetaldehyde, 33.3 μM NAD⁺, 10 mM DTT and 167 nM SmALDH_312. Each of the metal ions was tested individually in the concentration range 0.3–0.6 mM. We also assessed the effect of three different pH values (7.0, 8.5 and 10.0) and three different temperatures (25, 31.5 and 41°C). Based on these preliminary tests we investigated further promising ranges using a design-of-experiment (DoE) approach: pH 6.0–8.5 and temperatures of 41–45°C. The DoE model was prepared using Design Expert 11.1.2.0 (Stat-Ease, Minneapolis, MN, USA) and included a five-fold determination of center points with pH 7.25 at 43°C. Kinetic analysis was carried out for 2 h using 33.3 μM acetaldehyde, 33.3 μM NAD⁺, 10 mM DTT, 0.5 mM Mg²⁺ and 167 nM SmALDH_312. The specific activity after 2 h was set as the response. The reaction was maintained at pH 6.0 using the buffer 2-morpholinoethanesulfonic acid (MES) buffer and Tris-HCl buffer was used for the other values.

3. Results

3.1. Expression and purification of *E. coli*-derived SmALDH_312

Two *E. coli* strains (pLysS and LOBSTR-RIL) were transformed with the plasmid pET-30a-SmALDH_312. Following induction with IPTG, we detected a protein of the expected size (54 kDa) in the lysate of strain LOBSTR-RIL, and the quantity of this protein increased with cultivation time after induction (Fig. 4). We were able to detect SmALDH_312 in the LOBSTR-RIL strain already 1 h post induction with an increasing yield up to 4 h. The highest amount was observed 19 h post induction. We did not detect a corresponding protein in the lysate of strain pLysS, indicating that the production of SmALDH_312 in *E. coli* is strain-dependent. Therefore, we used the *E. coli* LOBSTR-RIL strain for further protein production.

SmALDH_312 produced in *E. coli* LOBSTR-RIL was not secreted to the supernatant and was therefore purified from the lysate of a 400 mL liquid culture by affinity chromatography, targeting the His₆ tag. The fractions were analyzed with SDS-PAGE (Fig. 5). A 54 kDa protein that was not present before induction (lane 1)

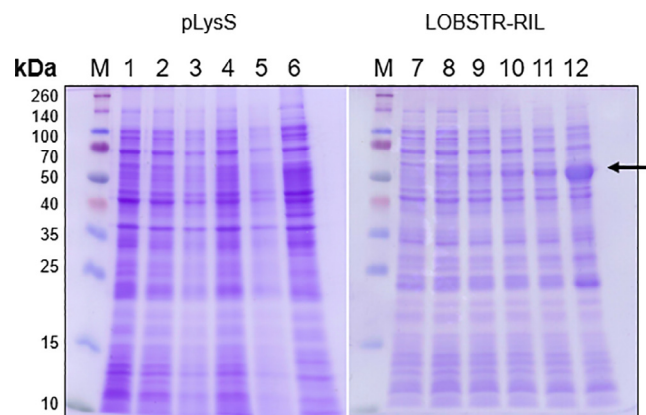


Fig. 4. Comparative SDS-PAGE analysis (Coomassie Brilliant Blue (CBB) stain) of SmALDH_312 production in *E. coli* strains pLysS (left) and LOBSTR-RIL (right). The product band with a molecular mass of ~54 kDa (arrow) was present only in the LOBSTR-RIL lysate. M = marker. Lanes 1, 7 = samples before induction. Lanes 2–5/8–11 = samples taken at hourly intervals post-induction. Lanes 6, 12 = samples taken 19 h post-induction.

was detected 4 h post-induction (lane 2). The protein was more abundant in the lysed bacterial pellet fraction (lane 3) than the recovered lysate fraction (lane 4), but the latter was sufficient to continue with affinity purification. The protein was eluted from the affinity column by increasing the concentration of imidazole. The elution fractions up to 100 mM imidazole (lanes 10–13) contained mostly host cell proteins, which were largely absent from subsequent fractions. Most of the target protein eluted in the 100–200 mM imidazole range (lanes 18–21). The subsequent elution fractions (up to 300 mM imidazole) contained residual amounts of the target protein and some host cell proteins. The purest fractions of SmALDH_312 (lanes 17–23) were pooled and concentrated before rebuffing.

3.2. Expression and purification of BEVS-derived SmALDH_312

The integration of the bacmid insert was confirmed by restriction analysis before the generation (P1) and amplification (P2) of a recombinant baculovirus stock in Sf-9 cells, which were then used for the production of SmALDH_312. To confirm the secretion of the product, we compared the Sf-9 supernatant and cell lysate by SDS-PAGE (CBB stain) and Western blot (Fig. 6). We detected bands with the expected molecular mass of ~56 kDa in the supernatant fractions and also in the lysate, and the identity of the protein was confirmed by Western blot using an antibody recognizing the His₆ tag. A slightly higher molecular weight was anticipated when using BEVS due to the presence of the signal peptide.

Culture supernatant (100 mL) of the BEVS-derived SmALDH_312 was purified by affinity chromatography as described for the same protein produced in *E. coli*. The fractions of BEVS-derived SmALDH_312 were analyzed by SDS-PAGE and western blot (Fig. 7). Bands of the anticipated molecular mass with the highest intensity were detected in the first three elution fractions (lanes 5–7), which were pooled for use in subsequent experiments. SmALDH_312 was also detected in the crude sample (lane 1), flow through (lane 2) and wash fractions (lanes 3 and 4), with low band intensity. This indicated that some protein was lost during purification.

3.3. Determination of protein concentration, recovery rate and purity

We determined the concentration of SmALDH_312 produced in the two expression systems using a BCA assay. Due to the high amount of unspecific proteins, originating from *E. coli* and Sf-9

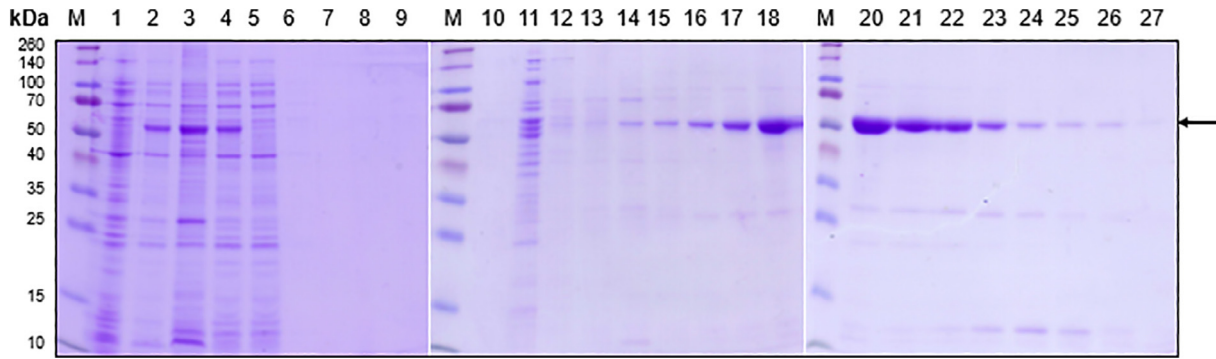


Fig. 5. SDS-PAGE analysis (CBB stain) for the detection of *E. coli*-derived SmALDH₃₁₂ (arrow) in the elution fractions of a His-trap affinity column. M = marker. Lane 1 = sample before induction (negative control). Lane 2 = harvest point. Lane 3 = lysed bacterial pellet. Lane 4 = lysate. Lanes 5, 6 = flow through. Lanes 7–9 = wash fractions. Lanes 10, 11 = elution up to 50 mM imidazole. Lanes 12, 13 = elution up to 100 mM imidazole. Lanes 14–17 = elution up to 150 mM imidazole. Lanes 18–21 = elution up to 200 mM imidazole. Lanes 22–25 = elution up to 300 mM imidazole. Lanes 26, 27 = elution with 300 mM imidazole.

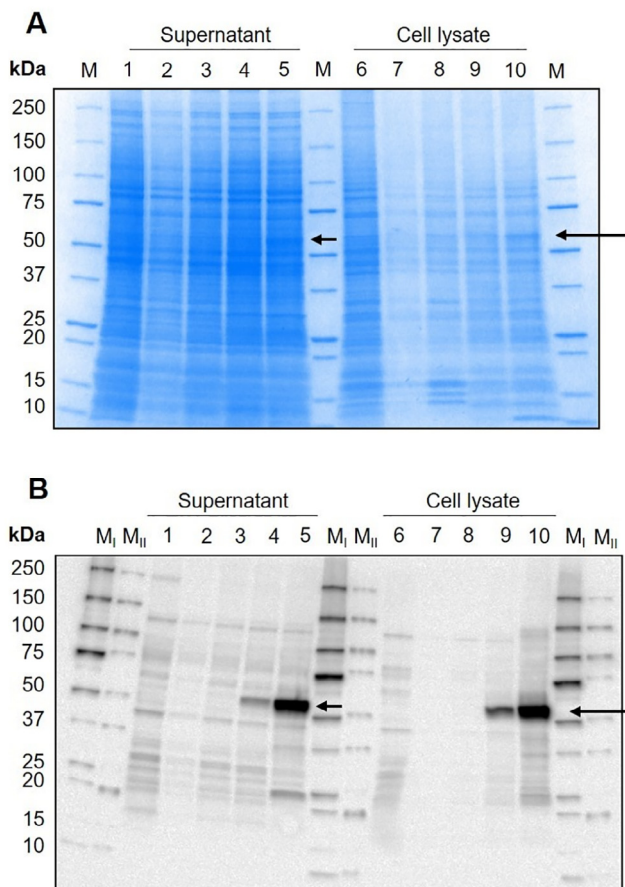


Fig. 6. (A) SDS-PAGE (CBB stain) and (B) Western blot analysis for the detection of secreted SmALDH₃₁₂ (56 kDa, arrow) produced in a 1 L shake flask culture of *Sf-9* cells (BEVS). M = marker. Lane 1 = control (supernatant). Lane 2–5 = samples of culture supernatant 0, 24, 48 and 72 h post-infection. Lane 6 = control cell lysate. Lanes 7–10 = samples of lysed cells 0, 24, 48 and 72 h post-infection.

cells, leading to invalid measurement results, the concentration of the target protein SmALDH₃₁₂ was determined after purification and buffer exchange. The concentration of the rebuffed 0.5-mL fraction of SmALDH₃₁₂ produced in *E. coli* was $147.2 \pm 2.18 \text{ mg}\cdot\text{L}^{-1}$, whereas that of the pooled fraction (1.5 mL) of BEVS-derived SmALDH₃₁₂ was $77.7 \pm 4.36 \text{ mg}\cdot\text{L}^{-1}$. Recovery of the BEVS-derived SmALDH₃₁₂ was 43.2% in the purification step and 77.5% in the buffer exchange step, leading to a total recovery of 33.5%. Recovery of the *E. coli*-derived SmALDH₃₁₂ was 80% in

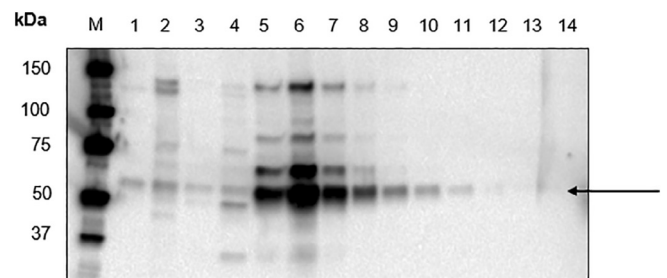


Fig. 7. Western blot analysis for the detection of BEVS-derived SmALDH₃₁₂ (56 kDa, arrow) in the elution fractions of a His-trap affinity column. M = marker. Lane 1 = crude sample (positive control). Lane 2 = flow through. Lanes 3, 4 = wash fractions. Lanes 5–14 = elution fractions up to 500 mM imidazole.

the purification step. After elution, the SmALDH₃₁₂ protein immediately started to precipitate. Consequently, the amount of unprecipitated protein to be rebuffed was decreased and furthermore, during rebuffing an additional part of the protein was lost. The recovery rate of SmALDH₃₁₂ after rebuffing was 1.73% and calculated overall protein recovery rate was 1.38%. Densitometric evaluation indicated that the SmALDH₃₁₂ fractions produced in *E. coli* and BEVS were 80.9% and 92.3% pure, respectively (Fig. 8).

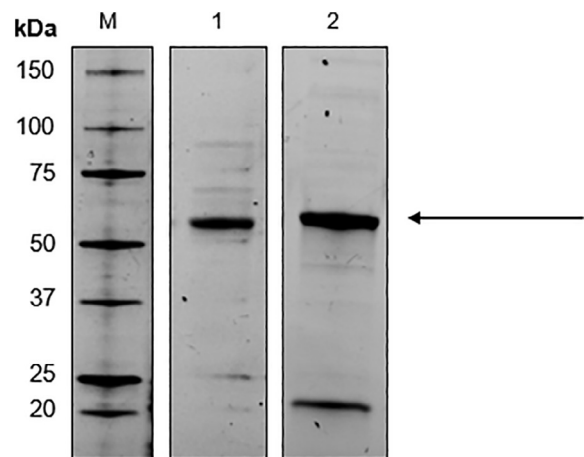


Fig. 8. SDS-PAGE (stain-free) of the pooled rebuffed fractions of SmALDH₃₁₂ produced in BEVS (lane 1) and the single rebuffed fraction produced in *E. coli* (lane 2) for verification of protein production and purity analysis. The expected product (~56 kDa) is indicated by an arrow. This figure was composed of 2 separate gels. M = marker.

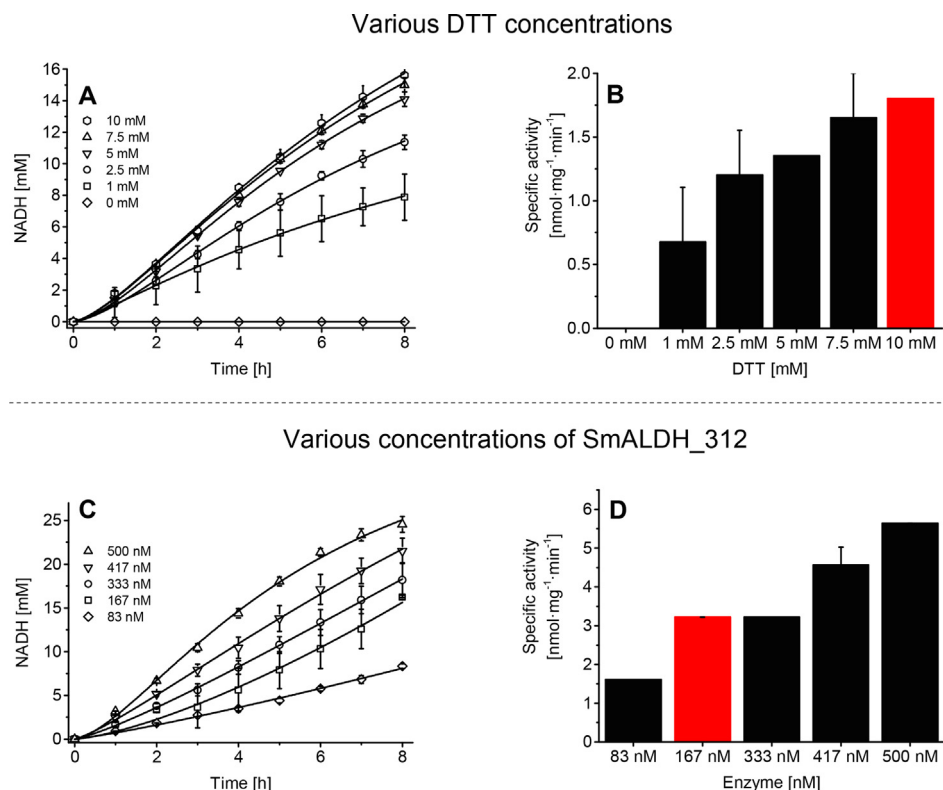


Fig. 9. Setup of the SmALDH_312 activity assay. (A, B) The influence of DTT concentration on NADH turnover, with the other parameters fixed at 167 nM SmALDH_312, 33.3 μM acetaldehyde and 33.3 μM NAD⁺. (C, D) The effect of different enzyme concentrations on specific enzyme activity, with the other parameters fixed at 100 μM acetaldehyde, 100 μM NAD⁺ and 10 mM DTT. Data are mean \pm standard errors (SEM), $n = 3$.

Given the higher purity but also the larger volume of the BEVS pooled fraction, the final concentration of the *E. coli* product was therefore 119.3 $\text{mg}\cdot\text{L}^{-1}$, and that of the BEVS product was 71.5 $\text{mg}\cdot\text{L}^{-1}$.

We showed that for the first time the schistosome ALDH_312 was recombinantly produced either with *E. coli* or BEVS. However, the *E. coli*-mediated expression depends on the *E. coli* strain and BEVS-mediated expression resulted in a higher relative purity of the recombinant SmALDH_312.

3.4. Determination of enzyme activity

In preliminary experiments, conducted with purified *E. coli*- and BEVS-derived SmALDH_312, the enzyme showed no activity. Human mitochondrial ALDH has a 57% similarity to SmALDH_312 and is only active under reduced conditions, so we tested the assay using BEVS-derived SmALDH_312 with different concentrations of DTT as a reducing agent. We observed the highest enzymatic activity of $1.8 \pm 0.0 \text{ U}\cdot\text{mg}^{-1}$ in the presence of 10 mM DTT (Fig. 9A, B). We also tested different concentrations of BEVS-derived SmALDH_312 and found that the specific enzyme activity generally correlated with the concentration but remained constant between 166 and 333 nM (Fig. 9C, D). Because we intend to use the enzyme in a screening assay for novel inhibitors, we committed to a concentration of 167 nM. At this concentration, the NADH turnover is sufficient to clearly distinguish between the active and inhibited forms of the enzyme. Accordingly, the final standard assay setup consisted of 167 nM SmALDH_312, 33.3 μM acetaldehyde, 33.3 μM NAD⁺ and 10 mM DTT.

Using the optimized assay setup, we compared the specific activities of SmALDH_312 produced in each of the expression systems. We found that the *E. coli*-derived enzyme reached a specific

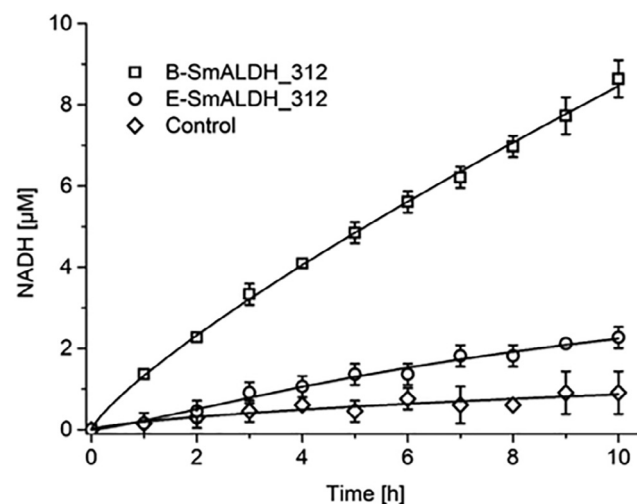


Fig. 10. Comparative activity of SmALDH_312 produced in *E. coli* (circle) and BEVS (square). Activity assays were carried out using 167 nM of each enzyme, 33.3 μM acetaldehyde, 33.3 μM NAD⁺ and 10 mM DTT. A control reaction was set up using SmALDH_312 from *E. coli* without DTT (diamond). Data are mean \pm standard errors (SEM), $n = 3$.

activity of $0.56 \pm 0.28 \text{ U}\cdot\text{mg}^{-1}$, with a maximum NADH turnover of $2.27 \pm 0.45 \mu\text{M}$ after 10 h, whereas the BEVS-derived enzyme reached a specific activity of $2.07 \pm 0.16 \text{ U}\cdot\text{mg}^{-1}$, with a maximum NADH turnover of $8.64 \pm 0.45 \mu\text{M}$ after 10 h (Fig. 10). The BEVS-derived SmALDH_312 showed a 3.7-fold higher enzymatic activity and 3.8-fold higher NADH turnover than its counterpart produced in *E. coli* and was therefore selected for more detailed characterization.

3.5. Further characterization of BEVS-derived SmALDH_312

3.5.1. Influence of metal ions

Aldehyde dehydrogenases often require divalent metal cations as cofactors, so we tested the effect of Mg^{2+} , Ca^{2+} and Mn^{2+} (concentration range 0.3–0.6 mM) on SmALDH_312 activity (Fig. 11). Mg^{2+} achieved the strongest effect, increasing enzyme activity by a maximum of 1.5-fold at a concentration of 0.5 mM. Ca^{2+} also exerted its strongest effect at 0.5 mM, although the increase in enzyme activity was only 1.3-fold. In contrast, the lowest tested concentration of Mn^{2+} (0.3 mM) induced the maximum 1.4-fold increase in enzyme activity, and higher concentrations had a weaker effect, although still increased enzyme activity over the baseline with no divalent cations. Interestingly, exposing the enzyme to higher concentrations of the other cations reduced its activity below the baseline, indicating that 0.6 mM Mg^{2+} and Ca^{2+} has an inhibitory effect. Based on these results, we selected 0.5 mM Mg^{2+} as the optimal divalent cation composition for enzyme activity in the kinetic characterization assays.

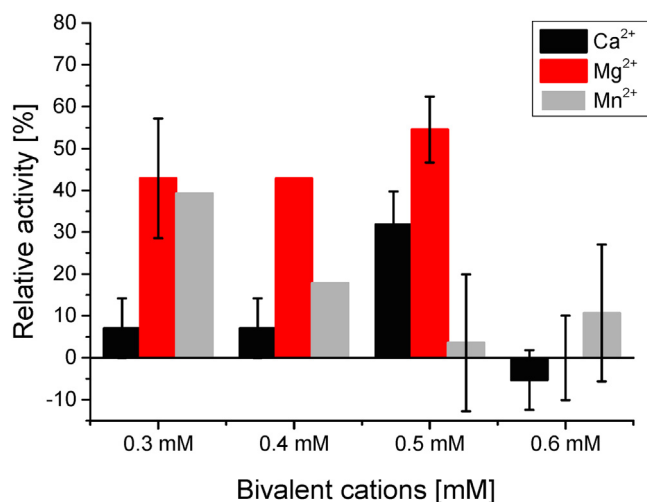


Fig. 11. Influence of divalent metal ions on the activity of SmALDH_312. The relative activity indicates the percentage increase/decrease in specific activity compared to the standard assay with no metal ions. Data are mean \pm standard errors (SEM), $n = 3$.

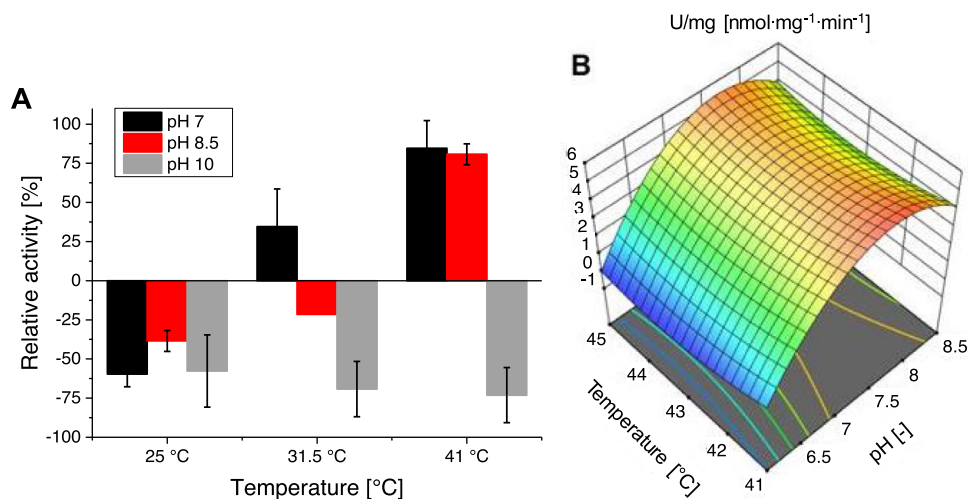


Fig. 12. Influence of pH and temperature on the activity of SmALDH_312. (A) Relative activity of SmALDH_312 at three pH values and three temperatures. The relative activity indicates the percentage increase/decrease in specific activity compared to the standard assay conditions (pH 7.5, 37°C). Data are mean \pm standard errors (SEM), $n = 3$. (B) Response surface model for the prediction of specific enzyme activity ($U \cdot mg^{-1}$) based on the factors pH [-] and temperature [°C].

3.5.2. Optimization of pH and temperature

To determine the optimal pH and temperature, preliminary tests were carried out to find the limits of the working range for both factors (Fig. 12A). At neutral to slightly alkaline pH, the enzyme activity increased with increasing temperature between 25 and 41°C. The maximum relative activity in each case as therefore observed at 41°C, representing increases of $84.6 \pm 17.6\%$ at pH 7.0 and $80.7 \pm 6.6\%$ at pH 8.0. In contrast, enzyme activity decreased with increasing temperature at pH 10.0. Given these results, we prepared a face centered central composite experimental design based on analysis of variance (ANOVA) to investigate higher temperatures up to 45°C. We also extended the pH range to 6.0. The model was found to be significant ($p < 0.0001$) whereas the lack of fit was not significant ($p = 0.1514$). The difference between the predicted R^2 (0.7836) and adjusted R^2 (0.9509) was < 0.2 . Furthermore, pH was a significant factor ($p < 0.0001$) but the interaction between pH and temperature was not significant. The model suggested that pH 7.6 and 41°C were the optimal reaction conditions, although the differences within the pH range 7.0–8.25 are minimal at 41°C suggesting this is a broad working range for the enzyme (Fig. 12B). The model also showed a decrease in specific activity between 42 and 44°C and further increase from 45°C that continued to the model limits.

To verify the model, we carried out a confirmation run at pH 7.6 and 41°C. Under these optimized conditions, we achieved a specific activity of $5.49 \pm 0.0 U \cdot mg^{-1}$, which was within the confidence interval (4.76–7.55). The pH and temperature optima led to a further 1.5-fold increase in the specific activity of SmALDH_312 compared to the standard assay conditions.

4. Discussion

The heterologous production of schistosome proteins can be challenging due to differences in base composition and codon preference between the source organism and host. The evaluation of different host systems can therefore help to optimize the expression of correctly folded and functional schistosome enzymes, especially for testing as potential drug targets. Here, we compared *E. coli* and BEVS for the production of SmALDH_312, a tegument protein from *S. mansoni*, which has not been expressed in a heterologous system before. We recognized a difference in the protein expression profiles using either *E. coli* strain pLysS, where no

expression was detected, or LOBSTR-RIL with additional rare codons for arginine, isoleucine and leucine, where protein was detected already 1 h post induction. Analysis of SmALDH_312 codons revealed a possible bottleneck for arginine tRNAs. However, codon usage cannot be the only reason for the different expression behavior of the *E. coli* strains. Even if codon optimized, 19 out of 94 expression constructs performed slightly weaker in a multi gene study. Furthermore, it was demonstrated that 21 constructs, (either wild type or optimized) showed no expression at all [10]. Therefore, in case of SmALDH_312 choosing the appropriate expression system was found to be important for successful protein production.

Although related enzymes such as human ALDH2 and ALDH3A1 have been expressed successfully [39,40], our study reports the first expression of recombinant SmALDH_312 using *E. coli* and BEVS. The practical differences between the platforms in terms of elution volumes and purification means it is uninformative to compare the yields, so we focus on the comparative functionality of SmALDH_312 produced using each system.

We found that SmALDH_312 produced in *E. coli* was considerably less active than its counterpart produced in the BEVS, as previously reported for β -1,4-endoglucanase [41]. In this earlier study, the authors speculated that the activity of bacterial product may have been limited by misfolding and/or the absence of PTMs. Misfolding may result from the inability of *E. coli* to form disulfide bonds in the cytoplasm and/or the saturation of the protein-folding machinery due to protein overexpression, in both cases leading to the formation of inclusion bodies [27,42]. Potential solutions include lowering the cultivation temperature (which slows down protein expression and allows the protein folding machinery to process nascent proteins correctly) and the expression of soluble target proteins, for example using a fusion partner [43,44]. Alternatively, the co-expression of chaperons can facilitate protein folding [45,46], as demonstrated in the case of human mitochondrial ALDH by the co-expression of His60 and His10 [47]. Furthermore, PTMs are involved in folding processes and may contribute to the stability and functionality of some enzymes [48]. Human ALDH2 and other members of the ALDH family are known to undergo acetylation and phosphorylation [49]. Across vertebrate species, conservation of lysine acetylation sites was demonstrated, and compared to mice, 87% of lysine acetylation sites of proteins were conserved in humans [50]. Phosphorylation events were described for human ALDH1A2 at tyrosines and serines [51]. Since acetylation and phosphorylation appeared to be the prominent PTMs in human ALDH, we analyzed the literature accordingly. In *S. mansoni*, a histone acetyltransferase paralogue (SmGCN5) was found and revealed acetylation at Lys-14 of histone 3, but also at the schistosome retinoid X receptor 1 [19]. In *S. japonicum*, 1109 proteins were found with acetylated lysines. Among these is the putative aldehyde dehydrogenase 1B1 (uniprot-ID: C1LFP4; NCBI Accession: CAX73522) harboring 6 acetylation sites. [52] Using NCBI's protein blast function, this amino acid sequence revealed a 100% match to SmALDH_312. Therefore, we assume that parts of these PTM sites are also conserved in *S. mansoni*. A recent study demonstrated 3,176 phosphorylated proteins in a broad-based phosphoproteome analysis in *S. mansoni*, in which phosphorylation was found to be dominant at serines (67.8%), followed by threonines (20.1%), and tyrosines (12.1%) [12]. Furthermore, incubation of *S. mansoni* adult worms with human tumor necrosis factor alpha led to induction of phosphorylation events of 8 serine, 9 threonine, and 5 tyrosine residues in SmALDH_312 [53]. As shown in a study of Nene et al. [54], phosphorylation of Ser-279 in human ALDH2 elevates the enzymatic activity. SmALDH_312 lacks Ser-279, but also shares Tyr-384, -412, and -433, as well as Ser-471. Tyr-384 was conserved in 16 of the 18 human ALDH isozymes, as Tyr-433 and Ser-471 were conserved in all 18 human ALDH isozymes. While phosphory-

lation of Tyr-412 led to an increased enzyme activity, it also protected ALDH2 from inhibition by 4-Hydroxynonenal, probably due to structural changes of the catalytic tunnel [54].

Taking these reported modifications together, we conclude that the observed difference between the activities of the SmALDH_312 enzymes recombinantly expressed in *E. coli* and insect cells can be explained by the capability introducing PTMs. It is known that *Sf*-9 cells introduce PTMs such as glycosylation, phosphorylation and acetylation in recombinant proteins [55]. In contrast, *E. coli* lacks certain modifications and is also limited in the amount of modifications compared to eukaryotes [56,57,58].

In addition to the intrinsic characteristics of the protein that contribute to enzyme activity, it is also necessary to investigate external factors such as substrate concentration, pH, and temperature. We found that the activity of SmALDH_312 is strongly pH-dependent, with a narrow pH working range of pH 7.0–8.25 and an optimum of pH 7.6. Many enzymes are characterized by a narrow pH range around the optimum value [59], and most members of the ALDH superfamily operate in the pH range 7.0–9.0 [60,61,62]. The pH-sensitivity of enzymes reflects the presence of amino acid groups that influence enzyme activity when ionized, hence the need to identify a precise pH optimum [59,63]. We also found that the activity of SmALDH_312 was highly dependent on the temperature, increasing as the temperature rises. The optimum temperature of an enzyme generally reflects an evolutionary adaptation to function at a specific location, which for *S. mansoni* would be the physiological body temperature of 37°C within the mesenteric veins of its human host. However, we found SmALDH_312 as more active at 41°C than 37°C, and maintained its activity up to at least 45°C (the highest temperature we tested, suggesting it may remain active at even higher temperatures). It is unclear why SmALDH_312 becomes more active at temperatures above those found at its typical site of action, but this appears to be a common phenomenon in the ALDH superfamily. For example, the temperature optimum for human salivary ALDH is 45°C despite the physiological temperature of 37°C in its typical location [64].

Metal ions are known to promote ALDH activity in some species [65,66] and Mg^{2+} plays a pivotal role in the activation of class 2 enzymes by directly facilitating the rate-limiting deacylation step of the reaction [67,68]. We therefore tested the effect of Mg^{2+} , Ca^{2+} and Mn^{2+} on the activity of the SmALDH_312, and found that 0.5 mM Mg^{2+} achieved the greatest increase in relative enzyme activity (1.7-fold) which is slightly below the 2-fold increase reported in other studies [65,67]. Furthermore, increasing the concentration of Mg^{2+} only slightly to 0.6 mM resulted in a clear inhibitory effect, perhaps reflecting the slower dissolution of NADH from the enzyme, or coenzyme dissociation [67].

5. Conclusions

We compared two widely used expression systems for the development of a platform that allows the high-level expression of functional schistosome enzymes for screening as putative drug targets. Although *E. coli* has many advantages, such as rapid expression, high yields, and low costs, this system was outperformed by BEVS for the production of a schistosome ALDH. The expression of SmALDH_312 requires PTMs such as phosphorylation, and perhaps also acetylation at sites that are possibly not modified by *E. coli*. Alternatively, the production of stable and soluble SmALDH_312 may benefit from the protein folding environment of the insect cells, making BEVS the most suitable platform for the production of this enzyme. Further results expressing the Abelson protein-tyrosine kinase 2 of *S. mansoni* (GeneID: Smp_128790) support the view that BEVS may be a generally suitable platform for the production of recombinant schistosome

enzymes. The availability of a functional recombinant SmALDH_312 allowed us to optimize the reaction kinetics in terms of pH, temperature, enzyme and substrate concentrations, and cofactor requirements. Having determined the optimal working range, it will be possible to establish the kinetic constants, which are required in turn for the screening assay to evaluate IC_{50} and k_i values. Our platform therefore provides an opportunity for the expression and subsequent evaluation of schistosome enzymes as drug targets.

Financial support

We would like to thank the Hessen State Ministry of Higher Education, Research and the Arts for the financial support within the Hessen Initiative for Scientific Economics Excellence (LOEWE-Program and LOEWE Center DRUID (Novel Drug Targets against Poverty-Related and Neglected Tropical Infectious Diseases)).

Conflict of interest

The authors declare that they have no known competing financial interests or personal relationships that could have appeared to influence the work reported in this paper.

Acknowledgments

We would like to thank A. Blohm for providing us the cloned SmALDH_312 construct, which was used for the expression in *E. coli*. The authors also acknowledge Dr. Richard M Twyman for revising the paper.

References

- [1] Ikemura T. Codon usage and tRNA content in unicellular organisms. *Mol Biol Evol* 1985;2(1):13–34. <https://doi.org/10.1093/oxfordjournals.molbev.a040335>. PMID:3916708.
- [2] Musto H, Cacciò S, Rodríguez-Maseda H, et al. Compositional constraints in the extremely GC-poor genome of *Plasmodium falciparum*. *Mem Inst Oswaldo Cruz* 1997;92(6):835–41. <https://doi.org/10.1590/s0074-02761997000600020>. PMID:9566216.
- [3] Gardner MJ, Hall N, Fung E, et al. Genome sequence of the human malaria parasite *Plasmodium falciparum*. *Nature* 2002;419(6906). <https://doi.org/10.1038/nature01097>. PMID:12368864.
- [4] Narum DL, Kumar S, Rogers WO, et al. Codon optimization of gene fragments encoding *Plasmodium falciparum* merozoite proteins enhances DNA vaccine protein expression and immunogenicity in mice. *Infect Immun* 2001;69(12):7250–3. <https://doi.org/10.1128/IAI.69.12.7250-7253.2001>. PMID:11705894.
- [5] Meadows HM, Simpson AJ. Codon usage in *Schistosoma*. *Mol Biochem Parasitol* 1989;36(3):291–3. [https://doi.org/10.1016/0166-6851\(89\)90178-3](https://doi.org/10.1016/0166-6851(89)90178-3). PMID:2797065.
- [6] Ellis J, Morrison DA, Kalinna B. Comparison of the patterns of codon usage and bias between *Brugia*, *Echinococcus*, *Onchocerca* and *Schistosoma* species. *Parasitol Res* 1995;81(5):388–93. <https://doi.org/10.1007/BF00931499>. PMID:7501637.
- [7] Protasio AV, Tsai IJ, Babbage A, et al. A systematically improved high quality genome and transcriptome of the human blood fluke *Schistosoma mansoni*. *PLoS Negl Trop Dis* 2012;6(1):. <https://doi.org/10.1371/journal.pntd.0001455>. PMID:22253936e1455.
- [8] Bolt BJ, Rodgers FH, Shafie M, et al. Using WormBase ParaSite: an integrated platform for exploring helminth genomic data. *Methods Mol Biol* 2018;1757:471–91. https://doi.org/10.1007/978-1-4939-7737-6_15. PMID:29761467.
- [9] Hamdan FF, Mousa A, Ribeiro P. Codon optimization improves heterologous expression of a *Schistosoma mansoni* cDNA in HEK293 cells. *Parasitol Res* 2002;88(6). <https://doi.org/10.1007/s00436-001-0585-0>. PMID:12107483.
- [10] Maertens B, Spriestersbach A, von Groll U, et al. Gene optimization mechanisms: a multi-gene study reveals a high success rate of full-length human proteins expressed in *Escherichia coli*. *Protein Sci* 2010;19(7):1312–26. <https://doi.org/10.1002/pro.408>. PMID:20506237.
- [11] Yu K, Yu Y, Tang X, et al. Transcriptome analyses of insect cells to facilitate baculovirus-insect expression. *Protein Cell* 2016;7(5):373–82. <https://doi.org/10.1007/s13238-016-0260-y>. PMID:27017378.
- [12] Hirst NL, Nebel J-C, Lawton SP, et al. Deep phosphoproteome analysis of *Schistosoma mansoni* leads development of a kinomic array that highlights sex-biased differences in adult worm protein phosphorylation. *PLoS Negl Trop Dis* 2020;14(3):. <https://doi.org/10.1371/journal.pntd.0008115>. PMID:32203512e0008115.
- [13] Smit CH, van Diepen A, Nguyen DL, et al. Glycomic analysis of life stages of the human parasite *Schistosoma mansoni* reveals developmental expression profiles of functional and antigenic glycan motifs. *Mol Cell Proteomics* 2015;14(7):1750–69. <https://doi.org/10.1074/mcp.M115.048280>. PMID:25883177.
- [14] Ziniel PD, Desai J, Cass CL, et al. Characterization of potential drug targets farnesyl diphosphate synthase and geranylgeranyl diphosphate synthase in *Schistosoma mansoni*. *Antimicrob Agents Chemother* 2013;57(12):5969–76. <https://doi.org/10.1128/AAC.00699-13>. PMID:24041901.
- [15] Pereira RV, Gomes MS, Olmo RP, et al. NEDD8 conjugation in *Schistosoma mansoni*: genome analysis and expression profiles. *Parasitol Int* 2013;62(2):199–207. <https://doi.org/10.1016/j.parint.2012.12.009>. PMID:23313772.
- [16] Costa MP, Oliveira VF, Pereira RV, et al. *In silico* analysis and developmental expression of ubiquitin-conjugating enzymes in *Schistosoma mansoni*. *Parasitol Res* 2015;114(5):1769–77. <https://doi.org/10.1007/s00436-015-4362-x>. PMID:25663106.
- [17] Pereira RV, Cabral FJ, Gomes MS, et al. Molecular characterization of SUMO E2 conjugation enzyme: differential expression profile in *Schistosoma mansoni*. *Parasitol Res* 2011;109(6):1537–46. <https://doi.org/10.1007/s00436-011-2394-4>. PMID:21573813.
- [18] Pereira RV, Cabral FJ, de Souza Gomes M, et al. Transcriptional profile and structural conservation of SUMO-specific proteases in *Schistosoma mansoni*. *J Parasitol Res* 2012;2012:.. <https://doi.org/10.1155/2012/480824>. PMID:23125916480824.
- [19] de Moraes Maciel R, Da Costa RFM, de Oliveira FMB, et al. Protein acetylation sites mediated by *Schistosoma mansoni* GCN5. *Biochem Biophys Res Commun* 2008;370(1):53–6. <https://doi.org/10.1016/j.bbrc.2008.03.022>. PMID:18346457.
- [20] Jortzik E, Wang L, Becker K. Thiol-based posttranslational modifications in parasites. *Antioxid Redox Signal* 2012;17(4):657–73. <https://doi.org/10.1089/ars.2011.4266>. PMID:22085115.
- [21] Haque SJ, Majumdar T, Barik S. Redox-assisted protein folding systems in eukaryotic parasites. *Antioxid Redox Signal* 2012;17(4):674–83. <https://doi.org/10.1089/ars.2011.4433>. PMID:22122448.
- [22] Arnér ES, Holmgren A. Physiological functions of thioredoxin and thioredoxin reductase. *Eur J Biochem* 2000;267(20):6102–9. <https://doi.org/10.1046/j.1432-1327.2000.01701.x>. PMID:11012661.
- [23] Colley DG, Bustinduy AL, Secor WE, et al. Human schistosomiasis. *The Lancet* 2014;383(9936):2253–64. [https://doi.org/10.1016/S0140-6736\(13\)61949-2](https://doi.org/10.1016/S0140-6736(13)61949-2). PMID:24698483.
- [24] Hotez P, Aksoy S. PLOS Neglected Tropical Diseases: Ten years of progress in neglected tropical disease control and elimination More or less. *PLoS Negl Trop Dis* 2017;11(4):. <https://doi.org/10.1371/journal.pntd.0005355>. PMID:28426662e0005355.
- [25] Lo NC, Addiss DG, Hotez PJ et al. A call to strengthen the global strategy against schistosomiasis and soil-transmitted helminthiasis: the time is now. *The Lancet Infect Dis* 2017;17(2). [https://doi.org/10.1016/S1473-3099\(16\)30535-7](https://doi.org/10.1016/S1473-3099(16)30535-7). PMID:27914852.
- [26] Walker AJ. Insights into the functional biology of schistosomes. *Parasit Vectors* 2011;4:203. <https://doi.org/10.1186/1756-3305-4-203>. PMID:22013990.
- [27] Rosano GL, Ceccarelli EA. Recombinant protein expression in *Escherichia coli*: advances and challenges. *Front Microbiol* 2014;5:172. <https://doi.org/10.3389/fmicb.2014.00172>. PMID:24860555.
- [28] Liu J, Dyer DH, Cheng J, et al. Aldose reductase from *Schistosoma japonicum*: crystallization and structure-based inhibitor screening for discovering antischistosomal lead compounds. *Parasit Vectors* 2013;6:162. <https://doi.org/10.1186/1756-3305-6-162>. PMID:23734964.
- [29] Shen J, Xu L, Liu Z, et al. Gene expression profile of LPS-stimulated dendritic cells induced by a recombinant Sj16 (rSj16) derived from *Schistosoma japonicum*. *Parasitol Res* 2014;113(8):3073–83. <https://doi.org/10.1007/s00436-014-3973-y>. PMID:24906993.
- [30] Bernardes WP, Araújo JM de, Carvalho GB et al. Sm16, A *Schistosoma mansoni* immunomodulatory protein, fails to elicit a protective immune response and does not have an essential role in parasite survival in the definitive host. *J Immunol Res* 2019;2019:6793596. <https://doi.org/10.1155/2019/6793596>. PMID:31886307.
- [31] Beckmann S, Quack T, Dissous C, et al. Discovery of plathyhelminth-specific α/β -integrin families and evidence for their role in reproduction in *Schistosoma mansoni*. *PLoS ONE* 2012;7(12):. <https://doi.org/10.1371/journal.pone.0052519>. PMID:23300694e52519.
- [32] Parker-Manuel RP, Grevelding CG, Gelmedin V. Cryptic 3' mRNA processing signals hinder the expression of *Schistosoma mansoni* integrins in yeast. *Mol Biochem Parasitol* 2015;199(1–2):51–7. <https://doi.org/10.1016/j.molbiopara.2015.03.005>. PMID:25827755.
- [33] Owczarek B, Gerszberg A, Hnatuszko-Konka K. A brief reminder of systems of production and chromatography-based recovery of recombinant protein biopharmaceuticals. *Biomed Res Int* 2019;2019. <https://doi.org/10.1155/2019/4216060>. PMID:30729123.
- [34] Liu F, Wu X, Li L, et al. Use of baculovirus expression system for generation of virus-like particles: successes and challenges. *Protein Expr Purif* 2013;90(2):104–16. <https://doi.org/10.1016/j.pep.2013.05.009>. PMID:23742819.
- [35] Hota-Mitchell S, Siddiqui AA, Dekaban GA, et al. Protection against *Schistosoma mansoni* infection with a recombinant baculovirus-expressed subunit of

- calpain. *Vaccine* 1997;15(15). [https://doi.org/10.1016/s0264-410x\(97\)00081-9](https://doi.org/10.1016/s0264-410x(97)00081-9). PMID:9364694.
- [36] Krautz-Peterson G, Debatis M, Tremblay JM, et al. *Schistosoma mansoni* infection of mice, rats and humans elicits a strong antibody response to a limited number of reduction-sensitive epitopes on five major tegumental membrane proteins. *PLoS Negl Trop Dis* 2017;11(1):. <https://doi.org/10.1371/journal.pntd.0005306>. PMID:28095417e0005306.
- [37] Ludolf F, Patrocínio PR, Corrêa-Oliveira R, et al. Serological screening of the *Schistosoma mansoni* adult worm proteome. *PLoS Negl Trop Dis* 2014;8(3):. <https://doi.org/10.1371/journal.pntd.0002745>. PMID:24651847e2745.
- [38] Sung L-Y, Chen C-L, Lin S-Y, et al. Efficient gene delivery into cell lines and stem cells using baculovirus. *Nat Protoc* 2014;9(8):1882–99. <https://doi.org/10.1038/nprot.2014.130>. PMID:25010908.
- [39] Pappa A, Estey T, Manzer R et al. Human aldehyde dehydrogenase 3A1 (ALDH3A1): biochemical characterization and immunohistochemical localization in the cornea. *Biochem J* 2003;376(Pt 3). 10.1042/BJ20030810. PMID:12943535.
- [40] Ho T, Chang C, Wu J, Huang I, Tsai L, Lin J et al. Recombinant expression of aldehyde dehydrogenase 2 (ALDH2) in *Escherichia coli* Nissle 1917 for oral delivery in ALDH2-deficient individuals; 2019.
- [41] Zhou X, Kovaleva ES, Wu-Scharf D, et al. Production and characterization of a recombinant beta-1,4-endoglucanase (glycohydrolase family 9) from the termite *Reticulitermes flavipes*. *Arch Insect Biochem Physiol* 2010;74(3):147–62. <https://doi.org/10.1002/arch.20368>. PMID:20572126.
- [42] Hwang PM, Pan JS, Sykes BD. Targeted expression, purification, and cleavage of fusion proteins from inclusion bodies in *Escherichia coli*. *FEBS Lett* 2014;588(2):247–52. <https://doi.org/10.1016/j.febslet.2013.09.028>. PMID:24076468.
- [43] Gopal GJ, Kumar A. Strategies for the production of recombinant protein in *Escherichia coli*. *Protein J* 2013;32(6). <https://doi.org/10.1007/s10930-013-9502-5>. PMID:23897421.
- [44] Costa S, Almeida A, Castro A, et al. Fusion tags for protein solubility, purification and immunogenicity in *Escherichia coli*: the novel Fh8 system. *Front Microbiol* 2014;5:63. <https://doi.org/10.3389/fmicb.2014.00063>. PMID:24600443.
- [45] Liu L, Yang H, Shin H, et al. How to achieve high-level expression of microbial enzymes: strategies and perspectives. *Bioengineered* 2013;4(4):212–23. <https://doi.org/10.4161/bioe.24761>. PMID:23686280.
- [46] Sadeghian-Rizi T, Ebrahimi A, Moazzen F, et al. Improvement of solubility and yield of recombinant protein expression in *E. coli* using a two-step system. *Res Pharm Sci* 2019;14(5):400–7. <https://doi.org/10.4103/1735-5362.268200>. PMID:31798656.
- [47] Gueldner J, Sayes C. Emerging associations of the ALDH2*2 polymorphism with disease susceptibility. *J Drug Metab Toxicol* 2016;7(2). <https://doi.org/10.4172/2157-7609.1000202>.
- [48] Ryšlavá H, Doubnerová V, Kavan D, et al. Effect of posttranslational modifications on enzyme function and assembly. *J Proteomics* 2013;92:80–109. <https://doi.org/10.1016/j.jpro.2013.03.025>. PMID:23603109.
- [49] Song B-J, Abdelmegeed MA, Yoo S-H, et al. Post-translational modifications of mitochondrial aldehyde dehydrogenase and biomedical implications. *J Proteomics* 2011;74(12):2691–702. <https://doi.org/10.1016/j.jpro.2011.05.013>. PMID:21609791.
- [50] Rardin MJ, Newman JC, Held JM, et al. Label-free quantitative proteomics of the lysine acetylome in mitochondria identifies substrates of SIRT3 in metabolic pathways. *PNAS* 2013;110(16):6601–6. <https://doi.org/10.1073/pnas.1302961110>. PMID:23576753.
- [51] Zhou H, Di Palma S, Preisinger C, et al. Toward a comprehensive characterization of a human cancer cell phosphoproteome. *J Proteome Res* 2013;12(1):260–71. <https://doi.org/10.1021/pr300630k>. PMID:23186163.
- [52] Hong Y, Cao X, Han Q, et al. Proteome-wide analysis of lysine acetylation in adult *Schistosoma japonicum* worm. *J Proteomics* 2016;148:202–12. <https://doi.org/10.1016/j.jpro.2016.08.008>. PMID:27535354.
- [53] Oliveira KC, Carvalho MLP, Bonatto JMC, et al. Human TNF- α induces differential protein phosphorylation in *Schistosoma mansoni* adult male worms. *Parasitol Res* 2016;115(2):817–28. <https://doi.org/10.1007/s00436-015-4812-5>. PMID:26547565.
- [54] Nene A, Chen C-H, Disatnik M-H, et al. Aldehyde dehydrogenase 2 activation and coevolution of its ePKC-mediated phosphorylation sites. *J Biomed Sci* 2017;24(1):3. <https://doi.org/10.1186/s12929-016-0312-x>. PMID:28056995.
- [55] Drugmand J-C, Schneider Y-J, Agathos SN. Insect cells as factories for biomanufacturing. *Biotechnol Adv* 2012;30(5):1140–57. <https://doi.org/10.1016/j.biotechadv.2011.09.014>. PMID:21983546.
- [56] Zhang J, Sprung R, Pei J, et al. Lysine acetylation is a highly abundant and evolutionarily conserved modification in *Escherichia coli*. *Mol Cell Proteomics* 2009;8(2):215–25. <https://doi.org/10.1074/mcp.M800187-MCP200>. PMID:18723842.
- [57] Macek B, Gnad F, Soufi B, et al. Phosphoproteome analysis of *E. coli* reveals evolutionary conservation of bacterial Ser/Thr/Tyr phosphorylation. *Mol Cell Proteomics* 2008;7(2):299–307. <https://doi.org/10.1074/mcp.M700311-MCP200>. PMID:17938405.
- [58] Macek B, Forchhammer K, Hardouin J, et al. Protein post-translational modifications in bacteria. *Nat Rev Microbiol* 2019;17(11):651–64. <https://doi.org/10.1038/s41579-019-0243-0>. PMID:31485032.
- [59] Bowman L, Motamed R, Lee P, et al. A simple and reliable method for determination of optimum pH in coupled enzyme assays. *Biotechniques* 2020;68(4):200–3. <https://doi.org/10.2144/btn-2019-0126>. PMID:32056453.
- [60] Lyu Y, LaPointe G, Zhong L et al. Heterologous expression of aldehyde dehydrogenase in *Lactococcus lactis* for acetaldehyde detoxification at low pH. *Appl Biochem Biotechnol* 2018;184(2). 10.1007/s12010-017-2573-6. PMID:28791590.
- [61] Aquino Neto S, Forti JC, Zucolotto V, et al. The kinetic behavior of dehydrogenase enzymes in solution and immobilized onto nanostructured carbon platforms. *Process Biochem* 2011;46(12):2347–52. <https://doi.org/10.1016/j.procbio.2011.09.019>.
- [62] Liu T, Hao L, Wang R et al. Molecular characterization of a thermostable aldehyde dehydrogenase (ALDH) from the hyperthermophilic archaeon *Sulfolobus tokodaii* strain 7. *Extremophiles* 2013;17(1). 10.1007/s00792-012-0503-7. PMID:23224332.
- [63] Rostkowski M, Olsson MHM, Søndergaard CR, et al. Graphical analysis of pH-dependent properties of proteins predicted using PROPKA. *BMC Struct Biol* 2011;11:6. <https://doi.org/10.1186/1472-6807-11-6>. PMID:21269479.
- [64] Alam MF, Laskar AA, Choudhary HH, et al. Human salivary aldehyde dehydrogenase: purification, kinetic characterization and effect of ethanol, hydrogen peroxide and sodium dodecyl sulfate on the activity of the enzyme. *Cell Biochem Biophys* 2016;74(3):307–15. <https://doi.org/10.1007/s12013-016-0742-9>. PMID:27324040.
- [65] Weiner H, Takahashi K. Effects of magnesium and calcium on mitochondrial and cytosolic liver aldehyde dehydrogenases. *Pharmacol Biochem Behav* 1983;18:109–12. [https://doi.org/10.1016/0091-3057\(83\)90155-7](https://doi.org/10.1016/0091-3057(83)90155-7). PMID:6634825.
- [66] Gonnella TP, Leedahl TS, Karlstad JP, et al. NADH fluorescence lifetime analysis of the effect of magnesium ions on ALDH2. *Chem Biol Interact* 2011;191(1):147–52. <https://doi.org/10.1016/j.cbi.2011.01.023>. PMID:21276780.
- [67] Ho KK, Allali-Hassani A, Hurley TD, et al. Differential effects of Mg²⁺ ions on the individual kinetic steps of human cytosolic and mitochondrial aldehyde dehydrogenases. *Biochemistry* 2005;44(22):8022–9. <https://doi.org/10.1021/bi050038u>. PMID:15924421.
- [68] Belmont-Díaz JA, Yoval-Sánchez B, Calleja-Castañeda LF, et al. Alda-1 modulates the kinetic properties of mitochondrial aldehyde dehydrogenase (ALDH2). *FEBS J* 2016;283(19):3637–50. <https://doi.org/10.1111/febs.13833>. PMID:27521998.